**This is the accepted version of the following article: Örbom, Anders, et al. "Intratumoral Distribution of [177Lu] Lu-PSMA-617 Over Time and in Relation to Diagnostic Tracers in Animal Models of Prostate Cancer." *Cancer Biotherapy & Radiopharmaceuticals* (2024), which has now been formally published in final form at Cancer Biotherapy & Radiopharmaceuticals at https://doi.org/10.1089/cbr.2024.0170. This original submission version of the article may be used for non-commercial purposes in accordance with the Mary Ann Liebert, Inc., publishers' self-archiving terms and conditions.**

# Intratumoral distribution of [$^{177}$Lu]Lu-PSMA-617 over time and in relation to diagnostic tracers in animal models of prostate cancer

Anders Örbom[1*†], Joanna Strand[1], Mohamed Altai[1], Wahed Zedan[1], Amanda Kristiansson[1,2,3], Jens Ceder[1], Oskar Vilhelmsson Timmermand[1*]

*These authors contributed equally to this work and share first and last authorship

†Corresponding author

1. Department of Clinical Sciences Lund, Section for Oncology, Lund University, Lund, Sweden

2. Department of Clinical Sciences Lund, Section for Pediatrics, Lund University, Lund, Sweden

3. Department of Neonatology, Skåne University Hospital, Lund, Sweden

**Running title**

Intratumoral distribution of [$^{177}$Lu]Lu-PSMA-617

**Corresponding author**

Anders Örbom

Department of oncology, Lund University

Barngatan 4, 222 42 Lund

Sweden

anders.orbom@med.lu.se

+46704254058

**Keywords**

PSMA, intratumoral distribution, autoradiography, prostate cancer

## Abstract

### Introduction

Prostate-specific membrane antigen (PSMA) is a target for diagnostic PET-tracers and radiopharmaceutical therapy (RPT), e.g. [$^{177}$Lu]Lu-PSMA-617, in prostate cancer. This autoradiography study investigates [$^{177}$Lu]Lu-PSMA-617 intratumoral distribution over time, compared to PSMA expression, proliferation (Ki67), and [$^{68}$Ga]Ga-PSMA-11, [$^{18}$F]F-PSMA-1007, [$^{18}$F]FDG and [$^{18}$F]Fluorocholine distribution. Mice with LNCaP, 22Rv1 or PC-3 PIP xenografts got [$^{177}$Lu]Lu-PSMA-617 iv. Sacrificed 1h p.i. if co-injected with diagnostic tracers, otherwise at 20 min, 1-2, 12, 24, 48, 72 h, or 2-3 weeks p.i. Cryosectioned tumors imaged by autoradiography, adjacent sections Ki67 or PSMA stained.

### Results

Heterogenous distribution of [$^{177}$Lu]Lu-PSMA-617 was seen 20 min p.i., with visible overlap between tumor cells, Ki67, PSMA and radioactivity at 1-2 h p.i. Strongest Ki67-correlation at 48h, which became negative at 72h and beyond with some Ki67+/PSMA+ low radioactivity areas. Uptake in necrotic tissue was only observed at 2-3 weeks p.i. PSMA-targeted tracers distributed identically to [$^{177}$Lu]Lu-PSMA-617 whereas other tracers only had some overlap.

### Conclusion

Regrowth of the tumor post [$^{177}$Lu]Lu-PSMA-617 administration creates Ki67+/PSMA+ areas that have no radioactivity uptake and need additional therapy fractions. The identical intratumoral distribution of [$^{177}$Lu]Lu-PSMA-617 and PSMA-targeted PET-tracers indicate that these will reveal the areas inside the tumor targeted by RPT at least at 1 h p.i.

## Introduction

Metastatic prostate cancer (PCa) poses a significant clinical challenge. In the STAMPEDE trial, the median failure free survival for patients with metastatic androgen sensitive PCa treated with androgen deprivation therapy (ADT) alone was 11.2 months[1]. PCa that develops resistance to ADT has even fewer options for therapy[2]. Radiopharmaceutical therapy (RPT) with prostate-specific membrane antigen (PSMA) targeting agents have had success in this patient group. Ligands targeting PSMA, almost all based on glutamine urea-lysine dimers, offer better tissue clearance and potentially better penetration of solid tumors than antibody based PSMA targeting[3]. PSMA is mostly restricted to benign and malignant prostatic tissue, but with expression in other tissues, mainly the kidney and salivary glands[4]. Expression has been correlated with PCa grade[5]. Lutetium-177 labeled PSMA-617 ([$^{177}$Lu]Lu-PSMA-617, Pluvicto™) is the first RPT ligand FDA- and EMA-approved for PSMA positive metastatic PCa[6, 7].

PSMA targeting can also be used for medical imaging; for lesion detection, staging, and treatment planning. Despite success in other cancers, and possible role in advanced/recurrent PCa, [$^{18}$F] Fluorodeoxyglucose ([$^{18}$F]FDG) performs poorly in early stages of PCa due to low glucose metabolism[8-10]. Carbon-11 labeled Choline or Flourine-18 labeled Fluorocholine ([$^{18}$F]FCH) PET can detect distant metastases with usefulness in detection of osseus disease, outperforming bonescan but less successful in detection of lymph node metastases[11]. Serum prostate specific antigen (PSA) levels and Choline uptake are positively correlated[12]. A benefit of PSMA positron emission tomography (PET) is the possibility of pairing it with PSMA RPT for PSMA expression validation and follow-up. Gallium-68 PSMA-11 ([$^{68}$Ga]Ga-PSMA-11) PET has been FDA-approved for [$^{177}$Lu]Lu-PSMA-617 patient selection and has high sensitivity and specificity compared to conventional imaging[13, 14]. Another PSMA specific PET agent, Flourine-18 PSMA-1007 ([$^{18}$F]F-PSMA-1007), possibly

has better lesion detection following biochemical recurrence than [$^{68}$Ga]Ga-PSMA-11 in patients with lower PSA levels[15]. The hepatobiliary, not urinary, excretion of [$^{18}$F]F-PSMA-1007 could increase the detection rate in the urinary tract area[16], and positron range and yield of Flourine-18 are beneficial for image quality, however, high non-specific bone uptake has been reported[17].

Tumor-killing in RPT is dependent on the absorbed dose and its distribution, which is a function of radioactivity distribution inside a tumor. A tool for imaging the distribution of radioactivity is autoradiography, which can provide µm-level activity distributions from *ex vivo* tumor samples[18, 19]. The RPT agent distribution in relation to tumor biology can change as the therapy progresses[20], and is dependent on properties of the agent, and the expression and distribution of the target. In the publication record there are no longitudinal investigations of the changes in intratumoral distribution of [$^{177}$Lu]Lu-PSMA-617. Any investigation is either a minor part of a larger study[21] and/or with PSMA-617 labelled with other radionuclides[22, 23].

The aim of this study is to investigate how [$^{177}$Lu]Lu-PSMA-617 distributes inside tumors in xenograft models of PCa using autoradiography, over time, in relation to PSMA expression, proliferation (Ki67) and in comparison to the distribution of diagnostic tracers. To find generalizable patterns, the investigation was performed using tumor cell lines with different levels of PSMA expression.

## Materials and methods

*Radiolabeling*

Radiolabeling was conducted as described by Kratochwil et al.[24]. Circa 430 MBq of non-carrier added Lutetium-177 (ITM GmbH, Garching, Germany), 30–40 MBq/µL, was mixed with 100 µL sterile 0.4 M sodium acetate solution, pH 5.5, and 1.25 µL 20% w/w ascorbic acid solution; thereafter, 1 µL of a 10 mM solution of PSMA-617 (ABX, Radeberg, Germany or MedChemExpress, Monmouth Junction, NJ, USA) was added. The solution was heated to and maintained at 95 °C on a shaker for 15 min. Samples, 1 µL, were taken for instant Thin Layer Chromatography (iTLC) at 0 and 15 min. Sodium citrate solution 0.2 M (mobile phase) was allowed to migrate up the iTLC strip. The strips were then analyzed on a phosphor imager system (Cyclone Plus Phosphor Imager, PerkinElmer, Inc., Waltham, MA, USA) together with a free Lutetium-177-only control. Removing the sample from the shaker and cooling it to room temperature terminated the reaction. A sterile 0.9% sodium chloride solution was added, and the radiotracer diluted (1:3 or 1:7), a sample for iTLC taken, and pH tested, before injections in mice. Radiochemical purity was always >99% and no further purification was done (see example, Figure Supplementary 1) the specific activity was 43 ± 3 MBq/nmol (n = 4).

*Cell culture*

LNCaP and 22Rv1 were purchased from American Type Culture Collection (Manassas, VA, USA). PC-3 PIP cells were provided by Professor Anna Orlova (Uppsala University, Uppsala, Sweden). Compared to LNCaP, 22Rv1 has significantly lower PSMA expression[25], and PC-3 PIP slightly higher[26]. Cells were cultured in RPMI 1640 medium (Thermo Scientific, Waltham, MA, USA) supplemented with 10% foetal bovine serum (Thermo Scientific) with 100 U/mL penicillin and 100 µg/mL streptomycin (Thermo Scientific). The

cells were maintained at 37°C, 5% $CO_2$, in a humidified incubator and were detached with trypsin-EDTA solution (Thermo Scientific) and regularly tested for Mycoplasma (Mycoplasmacheck, Eurofins Genomics, Ebersberg, Germany).

*Animal studies*

All experiments were conducted according to directions by the regional ethical committee for animal trials Malmö/Lund (Dnr: 04350-2020), and in compliance with the ARRIVE guidelines. BALB/c nude male (Janvier Labs, Le Genest-Saint-Isle, France) 7-8 weeks old were inoculated subcutaneously on their right flank with 200 µL of a 1:1 RPMI-1640 and Matrigel (BD Biosciences, San Jose, CA, USA) solution containing 4–6 million LNCaP (n=24), 22Rv1 (n=9) or PC-3 PIP cells (n=14). Animals per tumor cell type, time of sacrifice and co-injected tracers are detailed in Table 1. Animals sacrificed 1-2 h p.i were given 5-12 MBq [$^{177}$Lu]Lu-PSMA-617, partly not to excessive countrate while still obtaining enough signal when imaging mice co-injected with diagnostic tracers ([$^{18}$F]FDG or [$^{18}$F]FCH at 10-80 MBq per animal or 10-23 MBq [$^{18}$F]F-PSMA-1007 or 1-10 MBq [$^{68}$Ga]Ga-PSMA-11 ; Lund University Hospital, Lund, Sweden). The 22Rv2 tumors got 8-9 MBq [$^{177}$Lu]Lu-PSMA-617, if co-injected, or 20-52 MBq, if sacrificed 2 h p.i. Animals sacrificed 12-72 h p.i. were given 12-22 MBq [$^{177}$Lu]Lu-PSMA-617. Some LNCaP animals (n = 3) received 80 MBq of [$^{177}$Lu]Lu-PSMA-617 and were sacrificed 2-3 weeks p.i. to study longer therapy effect on [$^{177}$Lu]Lu-PSMA-617 distribution. After sacrifice the tumor was excised and embedded in Tissue-Tek® O.C.T™ compound (Sakura Finetek; Alphen aan den Rijn, The Netherlands), frozen on dry ice and cryosectioned at 10 µm. Some tumor size measurements were made, see Supplementary materials.

*Autoradiography*

Autoradiography employed a double-sided silicon strip detector (Biomolex Imager 700, Biomolex, Oslo, Norway) with 50 µm intrinsic spatial resolution[27]. For co-injections, counts from each radionuclide in the autoradiography images were separated using difference in half-lives.. One microscope slide at a time was imaged, duration set depending on samples, activity-level and half-life. E.g., several slides containing a short-lived radionuclide could each be imaged for as little as 120 minutes. For $^{177}$Lu-only samples, duration could be up to 44 hours. Instrument data contained coordinates, energy, and timestamp for each detected event. Events were sorted into different time periods and the ratio between these used to determine the radionuclide mix in each pixel. Software was developed in IDL 8.5 (NV5 Geospatial Solutions Inc, Broomfield, CO, USA) to reconstruct images and correct for dead or miscalibrated detector strips. Once imaged, the slide was taken for hematoxylin and eosin staining[28]. This study does not present any absolute activity data, as the radioactivity per pixel will depend on injected activity and our focus here is the relative distribution as it can be translated into models to calculate e.g. tumor control probability for different activities.

*Immunohistochemistry*

Autoradiography and immunohistochemistry sections were cryosectioned directly adjacent. Cryosections were dried for 15 min in 37°C and then fixed with 4% PFA. Endogen peroxidase activity was quenched for 5-10 min (REAL Peroxidase blocking solution, Agilent Technologies, Santa Clara, CA, USA). Sections were incubated in a humidity chamber with rabbit anti-Ki-67 mAb (Clone SP6, Thermo Fischer Scientific) or anti-PSMA (Abcam ab133579)[29] for 1 h at room temperature (RT). Incubation with horseradish peroxidase conjugated goat anti-rabbit F(ab)2 (111-036-045, Jackson ImmunoResearch Laboratories, Inc., West Grove, PA, USA) was performed at RT for 30 min. The stain was developed by adding 3,3′-Diaminobenzidine (Agilent Technologies) for 10 min. After counterstaining with

hematoxylin, dehydration and mounting with Pertex (Histolab, Gothenburg, Sweden), sections were imaged using an Axio Scan Z1 imager (Carl Zeiss AG, Oberkochen, Germany).

*Correlation analysis*

In all PC-3 PIP tumors the mean of the relative uptake (counts in pixel as the fraction of the maximum counts found in an in-section pixel) was quantified in regions-of-interest (ROIs), 0.18-3.02 $mm^2$, using ImageJ[30]. Identical ROIs in each corresponding Ki-67 stained slide were drawn using ZEN 3.5 blue edition (Carl Zeiss AG) and exported to ImageJ. Intensity of staining per nuclear area was determined using the Immunoratio plugin with default settings[31]. Statistical analysis (Pearson correlation and non-parametric Spearman's correlation) of the correlation between the two was performed for each timepoint post injection using IBM SPSS Statistics version 27 (IBM, Armonk, NY, USA). LNCaP tumors were similarly investigated, see supplementary material.

**Results**

*Distribution in relation to tumor histology*

Qualitative evaluation of uptake at 20 minutes p.i. in LNCaP xenografts revealed an uneven distribution with activity mainly located on the edges of the tumors and in thin rivulets inside (Fig. 1). At 1, 1.5 and 2 hours all xenograft types presented with a more even distribution as [$^{177}$Lu]Lu-PSMA-617 seem to have infiltrated into the tumor (Fig. 1, Suppl. 2A-B). Later, in PC-3 PIP, at 24, 48 and 72 hours p.i. and in LNCaP at 25 hours p.i. homogenous distributions can be seen in tumor-cell containing areas. This presents as high uptake in areas with high tumor cell density and vice versa (Fig. 1, Suppl. 2D), and no uptake in necrotic or connective tissue. There are however small tumor-cell containing areas, mostly on the edges, with very low uptake. At 2-3 weeks p.i. the LNCaP xenograft sections appear to be affected by therapy and areas where activity has located are now more necrotic or granulate, some even

hemochromatic (Fig. 1, Suppl. 2E). Throughout the section there are isolated islets containing non-necrotic tumor cells with very low or no uptake.

*Distribution in relation to Ki67 and PSMA*

Comparing adjacent stainings for proliferation (Ki67), in LNCaP and 22Rv1 tumors at 1-24 hours p.i. with imaged [$^{177}$Lu]Lu-PSMA-617 activity show that denser Ki67 expression-areas correspond to higher uptake (Fig. 2, Suppl. 3). However, there are still some small areas, within the tumor and not along the nodule edges, or in isolated tumor-tissue islet where the uptake is lower despite proliferative cells. Later, at 72 hours p.i. in PC-3 PIP, high-uptake areas are more likely to have less Ki67 staining (Fig. 2) an effect even more pronounced in LNCaP at later time points (2-3 weeks, Fig. Suppl. 3). This indicates, at least in PC-3 PIP, that it takes about 72 h from injection for the therapeutic effect to lower Ki67 expression.

The qualitative observations are further supported by quantitative ROI analysis in PC-3 PIP tumors. These yielded statistically significant Pearson Correlations between [$^{177}$Lu]Lu-PSMA-617 relative mean uptake and Ki67 staining intensity at 1, 12, and 48 hours p.i. (Table 2). The positive correlation was most pronounced at 48h, but there was also a negative correlation, although not statistically significant, at 72h.

There is a high and even expression of PSMA in the PC-3 PIP xenografts. PSMA expression and uptake in PC-3 PIP has good overlap at 1 hour p.i. (Fig. 3). This relationship is the same at 12 and 24 hours. However there are now small PSMA-positive areas corresponding to low [$^{177}$Lu]Lu-PSMA-617, primarily at the borders, similar to Ki67 and histology results. At 48 and 72 hours p.i. increasingly areas with lower uptake have dense PSMA staining (Fig. 3).

*Distribution in relation to diagnostic tracers*

Co-injections of [$^{177}$Lu]Lu-PSMA-617 with either [$^{18}$F]FDG or [$^{18}$F]FCH showed that both diagnostic tracers have uptake in tumor tissue. Neither are taken up in necrotic areas and both

seem to penetrate better into dense tumor tissue than PSMA-targeted agents. While [$^{177}$Lu]Lu-PSMA-617 seems to track quite well with Ki67-expressing tumor cells, both [$^{18}$F]FDG and [$^{18}$F]FCH accumulate in areas with connective or other types of tissue and lack of tumor cells (Fig. 4). Comparing [$^{177}$Lu]Lu-PSMA-617 and PSMA-targeted diagnostic tracers ([$^{68}$Ga]Ga-PSMA-11 and [$^{18}$F]F-PSMA-1007) we see an almost identical intratumoral distribution (Fig. 4, Suppl. 4).

## Discussion

In this study we present the trends seen in intratumoral distribution over time for [$^{177}$Lu]Lu-PSMA-617 and its co-localization with Ki67, PSMA expression and diagnostic tracers [$^{68}$Ga]Ga-PSMA-11, [$^{18}$F]F-PSMA-1007, [$^{18}$F]FDG and [$^{18}$F]FCH at 1h. This was investigated in tumors with low (22Rv1), high (LNCaP) and artificially high (PC-3 PIP) PSMA expression[25, 26]. Previous studies have focused on single timepoints and/or on PSMA-617 labeled with other radionuclides[22, 23]. We found that the initial distribution of [$^{177}$Lu]Lu-PSMA-617 is on the scale of hours and thereafter a slower process, affected by the therapeutic response and regrowth of the tumor, sets in. In PC-3 PIP, statistically significant positive correlations between Ki67 expression and [$^{177}$Lu]Lu-PSMA-617 distribution at earlier timepoints, clearly trends negative from 72 h p.i. and onwards. Although not statistically significant, it indicates a window of therapeutic effect approximately before 72 h p.i. if we can generalize these PC3-PIP results. At 72 h there are however already small areas containing viable cells and low [$^{177}$Lu]Lu-PSMA-617 uptake, and heavily treated LNCaP tumors contain pockets of regrowth at 2 or 3 weeks p.i. A negative correlation is also found between Ki67 expression and [$^{177}$Lu]Lu-PSMA-617at 2-3 weeks for LNCaP xenografts. These results, showing areas of regrowth, is in line with our recent research on externally irradiated LNCaP xenografts which pointed towards reinitiation of proliferation prior to relapse being visible in tumor volume measurements[32]. We find it implausible that apparent regrowth should be initially non-targeted areas that have later started expressing PSMA due to paracrine signaling from other cells. Such induced expression have only been shown in umbilical vein endothelial cells[33], and results in our previous studies show that, e.g. for PC-3 PIP cells, we have PSMA-expression across the whole tumor absent any therapy[34].

Wang et al[35] has performed autoradiography on samples from patients after radioguided surgery of primary PCa 18 hours p.i. of [$^{99m}$Tc]Tc-PSMA-I&S. They found a heterogeneous

distribution of PSMA expression and radioligand uptake. Although PC-3 PIP is a model with high PSMA expression, and e.g. the distribution could differ in orthotopic xenografts with higher perfusion[36] our data reveal a similar correlation between PSMA expression and radioligand as seen by Wang et al[35]. In Figure Supplementary 5 the connection between uptake, histology and PSMA and Ki67 expression at early and late timepoints in PC-3 PIP tumors is displayed. When staining for PSMA, we see areas expressing the target antigen but with low uptake already at 24 h p.i., and increasingly so with time. This PSMA-expression indicate that PSMA-targeted diagnostic tracers could be used to reveal parts of the tumor that would require repeated RPT to be treated. We show that the intratumoral distribution of PSMA-targeted diagnostic tracers match well with that of [$^{177}$Lu]Lu-PSMA-617 whereas [$^{18}$F]FDG and [$^{18}$F]FCH are located in both tumor, connective or other non-tumor tissue. It is known that the more disease specific PSMA-targeted tracers outperform [$^{18}$F]FDG and [$^{18}$F]FCH in PCa imaging[37]. Our results indicate that this is true also on the small scale. The observed slightly better penetration of [$^{18}$F]FDG and [$^{18}$F]FCH into densely packed areas of tumor cells compared to PSMA-targeted agents could be due to smaller molecular size. RPT is given in several fractions[38] as the injected activity is limited by acute hematotoxicity. Imaging agents such as [$^{68}$Ga]Ga-PSMA-11 and [$^{18}$F]F-PSMA-1007 could therefore potentially help optimize the timing of these fractions. A limitation is that we have used preclinical xenografts, not patient material, and observations of tumor regrowth in mice cannot be directly translated into clinical recommendations[39]. The benefit of this approach however is that we have been able to study intratumoral distribution of $^{177}$Lu]Lu-PSMA-617 at several different timepoints in the range of hours, days and weeks after administration.

We injected activities of [$^{177}$Lu]Lu-PSMA-617 to hit count-rates at the time of imaging within the limitations of the autoradiography system. It is however well known that the mole amount of tracer injected will affect the uptake and saturation of the tumor. Our general

observations still appear consistent over the ranges of amount of injected tracer, and still hold when e.g. examining only the PC-3 PIP data with a smaller activity range. Another limitation of this study is that the PSMA IHC method was only available to us for the PC-3 PIP xenografts, which have an engineered expression of PSMA[40]. However, expression is not much higher than for LNCaP and the results are in line with other published studies[26, 35] When co-injecting [$^{177}$Lu]Lu-PSMA-617 and PSMA-targeted diagnostic tracers, they could affect each other's uptake and distribution. Still, we saw no changes in the general pattern of [$^{177}$Lu]Lu-PSMA-617 uptake in those cases.

For RPT, the absorbed dose must be characterized on the scale of the path length of the radionuclide emission, mm for beta- and µm for alpha-emitters[41]. Calculation of the true absorbed dose requires knowledge of the intratumoral distribution of radioactivity, which *in vivo* gamma cameras and SPECT systems do not provide[42]. Autoradiography of preclinical models is a method to bridge this gap in knowledge to characterize the intratumoral distribution of a radioligand and use this information to help explain the biological effects of absorbed dose in patient tumors[43, 44]. The sizes and location of the tumor, the injected activity per mass and general biology will differ between human patients and animal models which is why the useful knowledge here is of the more general character, e.g. relative intratumoral distribution, rather than precise activity uptake etc. These relative intratumoral distributions can then be used in models of the disease to e.g. calculate tumor control probability for different injected activites[45].

## Conclusion

Our data show the temporal changes in [$^{177}$Lu]Lu-PSMA-617 intratumoral localization in PCa xenografts over time up to three weeks post administration. This data indicates a timeframe for the uptake, therapeutic and regrowth phases of [$^{177}$Lu]Lu-PSMA-617, all with different distribution patterns. We also show that PSMA-targeted diagnostic tracers,

[$^{68}$Ga]Ga-PSMA-11 and [$^{18}$F]F-PSMA-1007, distribute identically intratumorally to [$^{177}$Lu]Lu-PSMA-617 whereas both [$^{18}$F]FDG and [$^{18}$F]FCH have a less similar distribution.

**Acknowledgements**

Bo Holmqvist and ImaGene-iT AB for immunolabeling of PSMA. Lund University BioImaging Center for providing space and experimental resources. Sven-Erik Strand for valuable advice.

**Authorship contribution statement**

**Joanna Strand, Mohamed Altai, Wahed Zedan, Amanda Kristiansson, and Jens Ceder:** Methodology, Investigation, Resources and Writing - Original Draft. **Anders Örbom and Oskar Vilhelmsson Timmermand:** Methodology, Investigation, Resources, Writing - Original Draft, Conceptualization, Software, Validation, Writing - Review & Editing, Visualization, Supervision, Project administration, and Funding acquisition.

**Authors disclosure**

The authors have no relevant financial or non-financial interests to disclose.

**Funding statement**

This study was performed with support from The Prostate Cancer Association and Mrs. Berta Kamprad's Foundation.

**Ethics approval**

All experiments were conducted in accordance with relevant guidelines and regulations. The approval for the study was given by the Malmö/Lund Animal Experimentation Ethics Committee at the Lund district court (Dnr: 04350-2020 with the addition Dnr 5.8.18-07300/2021). The study was carried out in compliance with the ARRIVE guidelines

**References**


1. James ND, Spears MR, Clarke NW, et al. Survival with newly diagnosed metastatic prostate cancer in the "docetaxel era": data from 917 patients in the control arm of the STAMPEDE trial (MRC PR08, CRUK/06/019). *Eur Urol.* 2015;67(6):1028-1038; doi: 10.1016/j.eururo.2014.09.032
2. Shore ND, Antonarakis ES, Cookson MS, et al. Optimizing the role of androgen deprivation therapy in advanced prostate cancer: Challenges beyond the guidelines. *The Prostate.* 2020;80(6):527-544; doi: 10.1002/pros.23967
3. Debnath S, Zhou N, McLaughlin M, et al. PSMA-targeting imaging and theranostic agents—Current status and future perspective. *Int J Mol Sci.* 2022;23(3):1158; doi: 10.3390/ijms23031158
4. Kinoshita Y, Kuratsukuri K, Landas S, et al. Expression of prostate-specific membrane antigen in normal and malignant human tissues. *World J Surg.* 2006;30:628-636; doi: 10.1007/s00268-005-0544-5
5. Wright Jr GL, Haley C, Beckett ML, Schellhammer PF. Expression of prostate-specific membrane antigen in normal, benign, and malignant prostate tissues. *Urol Oncol.* 1995;1(1):18-28; doi: 10.1016/1078-1439(95)00002-y
6. Sartor O, De Bono J, Chi KN, et al. Lutetium-177–PSMA-617 for metastatic castration-resistant prostate cancer. *N Engl J Med.* 2021;385(12):1091-1103; doi: 10.1056/NEJMoa2107322

7. Fallah J, Agrawal S, Gittleman H, et al. FDA Approval Summary: Lutetium Lu 177 vipivotide tetraxetan for patients with metastatic castration-resistant prostate cancer. *Clin Cancer Res.* 2023;29(9):1651-1657; doi: 10.1158/1078-0432.CCR-22-2875

8. Chang C-H, Wu H-C, Tsai JJ, Shen Y-Y, Changlai S-P, Kao A. Detecting metastatic pelvic lymph nodes by 18F-2-deoxyglucose positron emission tomography in patients with prostate-specific antigen relapse after treatment for localized prostate cancer. *Urol Int.* 2003;70(4):311-315; doi: 10.1159/000070141

9. Jadvar H, Desai B, Ji L, et al. Baseline 18F-FDG PET/CT parameters as imaging biomarkers of overall survival in castrate-resistant metastatic prostate cancer. *J Nucl Med.* 2013;54(8):1195-1201; doi: 10.2967/jnumed.112.114116

10. Jadvar H, Velez EM, Desai B, Ji L, Colletti PM, Quinn DI. Prediction of time to hormonal treatment failure in metastatic castration-sensitive prostate cancer with 18F-FDG PET/CT. *J Nucl Med.* 2019;60(11):1524-1530; doi: 10.2967/jnumed.118.223263

11. Poulsen MH, Petersen H, Høilund-Carlsen PF, et al. Spine metastases in prostate cancer: comparison of technetium-99m-MDP whole-body bone scintigraphy,[18 F] choline positron emission tomography (PET)/computed tomography (CT) and [18 F] NaF PET/CT. *BJU Int.* 2014;114(6):818-823; doi: 10.1111/bju.12599

12. Krause B, Souvatzoglou M, Tuncel M, et al. The detection rate of [11 C] choline-PET/CT depends on the serum PSA-value in patients with biochemical recurrence of prostate cancer. *Eur J Nucl Med Mol Imaging.* 2008;35:18-23; doi: 10.1007/s00259-007-0581-4

13. Wang X, Wen Q, Zhang H, Ji B. Head-to-Head Comparison of 68Ga-PSMA-11 PET/CT and Multiparametric MRI for Pelvic Lymph Node Staging Prior to Radical

Prostatectomy in Patients With Intermediate to High-Risk Prostate Cancer: A Meta-Analysis. *Front Oncol.* 2021;11:737989; doi: 10.3389/fonc.2021.737989

14. Hicks RM, Simko JP, Westphalen AC, et al. Diagnostic accuracy of 68Ga-PSMA-11 PET/MRI compared with multiparametric MRI in the detection of prostate cancer. *Radiology.* 2018;289(3):730-737; doi: 10.1148/radiol.2018180788
15. Giesel FL, Knorr K, Spohn F, et al. Detection efficacy of 18F-PSMA-1007 PET/CT in 251 patients with biochemical recurrence of prostate cancer after radical prostatectomy. *J Nucl Med.* 2019;60(3):362-368; doi: 10.2967/jnumed.118.212233
16. Giesel FL, Hadaschik B, Cardinale J, et al. F-18 labelled PSMA-1007: biodistribution, radiation dosimetry and histopathological validation of tumor lesions in prostate cancer patients. *Eur J Nucl Med Mol Imaging.* 2017;44:678-688; doi: 10.1007/s00259-016-3573-4
17. Grünig H, Maurer A, Thali Y, et al. Focal unspecific bone uptake on [18 F]-PSMA-1007 PET: a multicenter retrospective evaluation of the distribution, frequency, and quantitative parameters of a potential pitfall in prostate cancer imaging. *Eur J Nucl Med Mol Imaging.* 2021;48:4483-4494; doi: 10.1007/s00259-021-05424-x
18. Solon E, Balani S, Lee F. Whole-body autoradiography in drug discovery. *Curr Drug Metab.* 2002;3(5):451-462; doi: 10.2174/1389200023337207
19. Tronchin S, Forster JC, Hickson K, Bezak E. Dosimetry in targeted alpha therapy. A systematic review: current findings and what is needed. *Phys Med Biol.* 2022;67(9):09TR01; doi: 10.1088/1361-6560/ac5fe0
20. Örbom A, Eriksson SE, Elgström E, et al. The intratumoral distribution of radiolabeled 177Lu-BR96 monoclonal antibodies changes in relation to tumor histology over time in a syngeneic rat colon carcinoma model. *J Nucl Med.* 2013;54(8):1404-1410; doi: 10.2967/jnumed.112.117028

21. Ruigrok EA, van Vliet N, Dalm SU, et al. Extensive preclinical evaluation of lutetium-177-labeled PSMA-specific tracers for prostate cancer radionuclide therapy. *Eur J Nucl Med Mol Imaging.* 2021;48:1339-1350; doi: 10.1007/s00259-020-05057-6

22. Han X-D, Liu C, Liu F, et al. 64Cu-PSMA-617: A novel PSMA-targeted radio-tracer for PET imaging in gastric adenocarcinoma xenografted mice model. *Oncotarget.* 2017;8(43):74159; doi: 10.18632/oncotarget.18276

23. Zhang H, Abou D, Lu P, et al. [18F]-Labeled PARP-1 PET imaging of PSMA targeted alpha particle radiotherapy response. *Sci Rep.* 2022;12(1):13034; doi: 10.1038/s41598-022-17460-0

24. Kratochwil C, Giesel FL, Stefanova M, et al. PSMA-targeted radionuclide therapy of metastatic castration-resistant prostate cancer with 177Lu-labeled PSMA-617. *J Nucl Med.* 2016;57(8):1170-1176; doi: 10.2967/jnumed.115.171397

25. Gorges TM, Riethdorf S, von Ahsen O, et al. Heterogeneous PSMA expression on circulating tumor cells-a potential basis for stratification and monitoring of PSMA-directed therapies in prostate cancer. *Oncotarget.* 2016;7(23):34930; doi: 10.18632/oncotarget.9004

26. Kiess AP, Minn I, Chen Y, et al. Auger radiopharmaceutical therapy targeting prostate-specific membrane antigen. *J Nucl Med.* 2015;56(9):1401-1407; doi: 10.2967/jnumed.115.155929

27. Örbom A, Ahlstedt J, Serén T, et al. Characterization of a double-sided silicon strip detector autoradiography system. *Med Phys.* 2015;42(2):575-584; doi: 10.1118/1.4905049

28. Fischer AH, Jacobson KA, Rose J, Zeller R. Hematoxylin and eosin staining of tissue and cell sections. *Cold spring harbor protocols.* 2008;2008(5):pdb. prot4986; doi: 10.1101/pdb.prot4986

29. Derks YH, Rijpkema M, Amatdjais-Groenen HI, et al. Photosensitizer-based multimodal PSMA-targeting ligands for intraoperative detection of prostate cancer. *Theranostics.* 2021;11(4):1527; doi: 10.7150/thno.52166

30. Schneider CA, Rasband WS, Eliceiri KW. NIH Image to ImageJ: 25 years of image analysis. *Nat Methods.* 2012;9(7):671-675; doi: 10.1038/nmeth.2089

31. Tuominen VJ, Ruotoistenmäki S, Viitanen A, Jumppanen M, Isola J. ImmunoRatio: a publicly available web application for quantitative image analysis of estrogen receptor (ER), progesterone receptor (PR), and Ki-67. *Breast Cancer Res.* 2010;12(4):1-12; doi: 10.1186/bcr2615

32. Kristiansson A, Ceberg C, Bjartell A, Ceder J, Timmermand OV. Investigating Ras homolog gene family member C (RhoC) and Ki67 expression following external beam radiation therapy show increased RhoC expression in relapsing prostate cancer xenografts. *Biochem Biophys Res Commun.* 2024;728:150324; doi: 10.1016/j.bbrc.2024.150324

33. Nguyen DP, Xiong PL, Liu H, et al. Induction of PSMA and Internalization of an Anti-PSMA mAb in the Vascular Compartment. *Mol Cancer Res.* 2016;14(11):1045-1053; doi: 10.1158/1541-7786.MCR-16-0193

34. Abouzayed A, Zedan W, Altai M, Strand J, Örbom A. Co-injection of anti-HER2 antibody Trastuzumab does not increase efficacy of [177Lu] Lu-PSMA-617 therapy in an animal model of prostate cancer. *Am J Nucl Med Mol Imaging.* 2023;13(3):107.

35. Wang H, Remke M, Horn T, et al. Heterogeneity of prostate-specific membrane antigen (PSMA) and PSMA-ligand uptake detection combining autoradiography and postoperative pathology in primary prostate cancer. EJNMMI Research. 2023/11/16 2023;13(1):99; doi: 10.1186/s13550-023-01044-8

36. Zhang W, Fan W, Rachagani S, et al. Comparative study of subcutaneous and orthotopic mouse models of prostate cancer: vascular perfusion, vasculature density, hypoxic burden and BB2r-targeting efficacy. *Sci Rep.* 2019;9(1):11117; doi: 10.1038/s41598-019-47308-z

37. Fraum TJ, Ludwig DR, Kim EH, Schroeder P, Hope TA, Ippolito JE. Prostate cancer PET tracers: essentials for the urologist. *Can J Urol.* 2018;25(4):9371-9383.

38. Rao DV, Howell RW. Time-dose-fractionation in radioimmunotherapy: implications for selecting radionuclides. *J Nucl Med.* 1993;34(10):1801-1810.

39. Brubaker DK, Lauffenburger DA. Translating preclinical models to humans. *Science.* 2020;367(6479):742-743; doi: 10.1126/science.aay8086

40. Current K, Meyer C, Magyar CE, et al. Investigating PSMA-Targeted Radioligand Therapy Efficacy as a Function of Cellular PSMA Levels and Intratumoral PSMA Heterogeneity. *Clin Cancer Res.* 2020;26(12):2946-2955; doi: 10.1158/1078-0432.CCR-19-1485

41. Roeske JC, Aydogan B, Bardies M, Humm JL. Small-scale dosimetry: challenges and future directions. *Semin Nucl Med.* 2008;38(5):367-383; doi: 10.1053/j.semnuclmed.2008.05.003

42. Jackson P, Hofman M, McIntosh L, Buteau JP, Kumar AR. Radiation dosimetry in 177Lu-PSMA-617 therapy. *Semin Nucl Med.* 2022;52(2):243-254; doi: 10.1053/j.semnuclmed.2021.11.003

43. Lassmann M, Eberlein U. The relevance of dosimetry in precision medicine. *J Nucl Med.* 2018;59(10):1494-1499; doi: 10.2967/jnumed.117.206649

44. Graves SA, Hobbs RF. Dosimetry for Optimized, Personalized Radiopharmaceutical Therapy. Semin Radiat Oncol. Jan 2021;31(1):37-44; doi: 10.1016/j.semradonc.2020.07.008

45. Mellhammar E, Dahlbom M, Vilhelmsson-Timmermand O, Strand S-E. Tumor Control Probability and Small-Scale Monte Carlo Dosimetry: Effects of Heterogenous Intratumoral Activity Distribution in Radiopharmaceutical Therapy. *J Nucl Med.* 2023;64(10):1632-1637; doi: 10.2967/jnumed.123.265523

## Tables

### TABLE 1. Number of animals per treatment

| | Time post injection of sacrifice | | | | | | | Co-injected tracer | | | | IHC | |
|---|---|---|---|---|---|---|---|---|---|---|---|---|---|
| Cell line | 20 min (n) | 1-2 h (n) | 12 h (n) | 24-25 h (n) | 48 h (n) | 72 h (n) | 2 -3 w (n) | [$^{18}$F] FDG (n) | [$^{18}$F] FCH (n) | [$^{69}$Ga]Ga -PSMA-11 (n) | [$^{18}$F]F-PSMA-1007 (n) | Ki67 | PSMA |
| LNCaP | 3 | 29 | - | 3 | | - | 3 | 12 | 9 | 3 | - | yes | no |
| PC-3 PIP | - | 3 | 3 | 2 | 3 | 3 | - | - | - | - | 3 | yes | yes |
| 22Rv1 | - | 9 | - | - | - | - | - | 3 | - | 1 | - | yes | No |

### TABLE 2. Correlation between relative [$^{177}$Lu]Lu-PSMA-617 uptake and fraction of cells with Ki67 staining in PC-3 PIP tumor sections

| Time post injection | 1 h | 12 h | 24 h | 48 h | 72 h |
|---|---|---|---|---|---|
| Number of ROIs analyzed | 11 | 13 | 12 | 13 | 14 |
| Pearson Correlation | 0.683* | 0.602* | 0.505 | 0.661* | -0.420 |
| Spearman's Correlation | 0.478 | 0.622* | 0.371 | 0.729* | -0.511 |

* Correlation is significant at the 0.05 level (2-tailed).

**Figures**

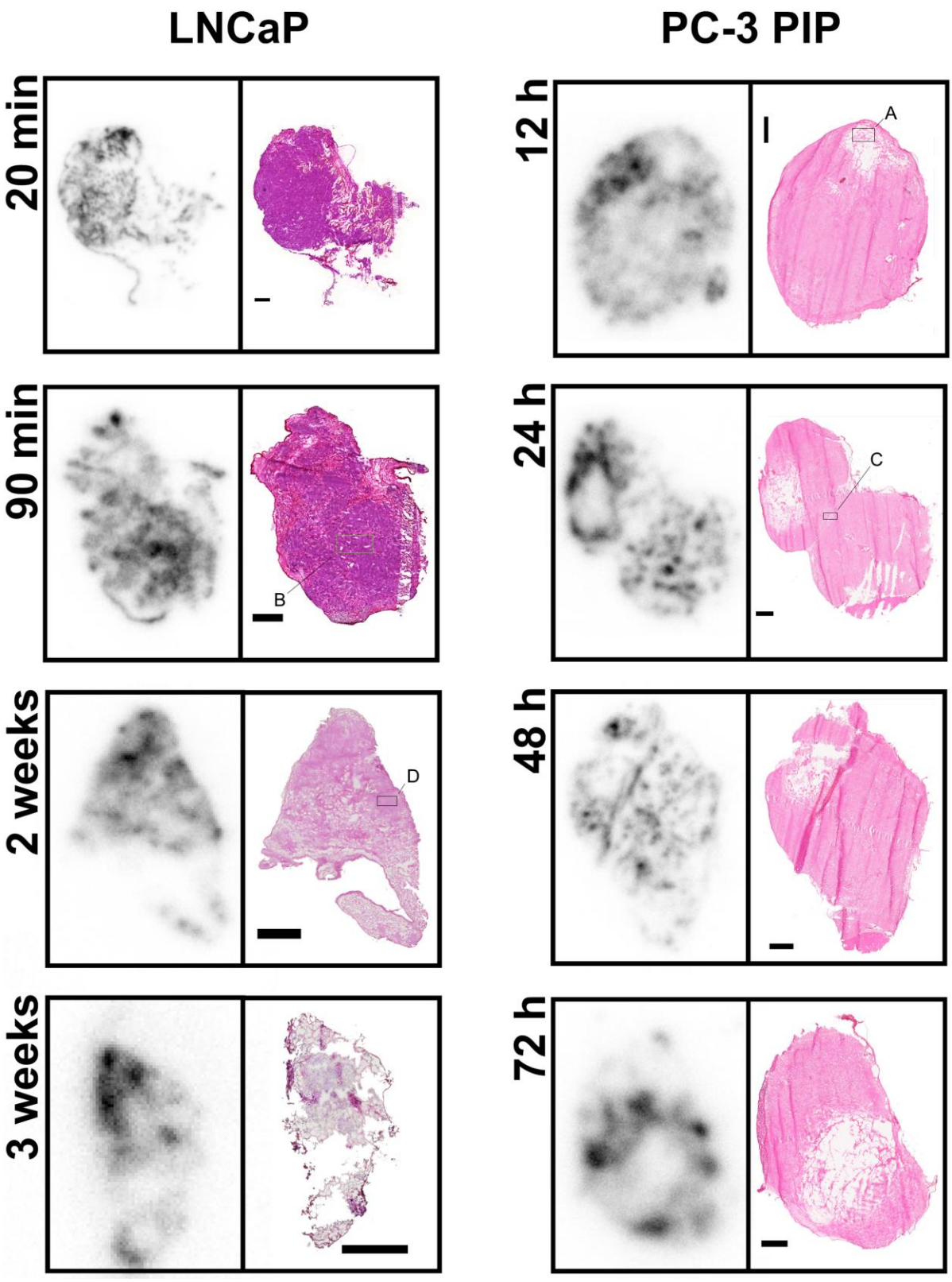


**FIGURE 1. Autoradiography and histology** Autoradiography of [$^{177}$Lu]Lu-PSMA-617 uptake (left), and H&E staining of histology in the same section (right). Labeled rectangles

represent areas magnified in Suppl. Fig 2E-H. All autoradiography images are individually scaled from zero (white) to max uptake (black) in that image. Black lines represent 1mm.

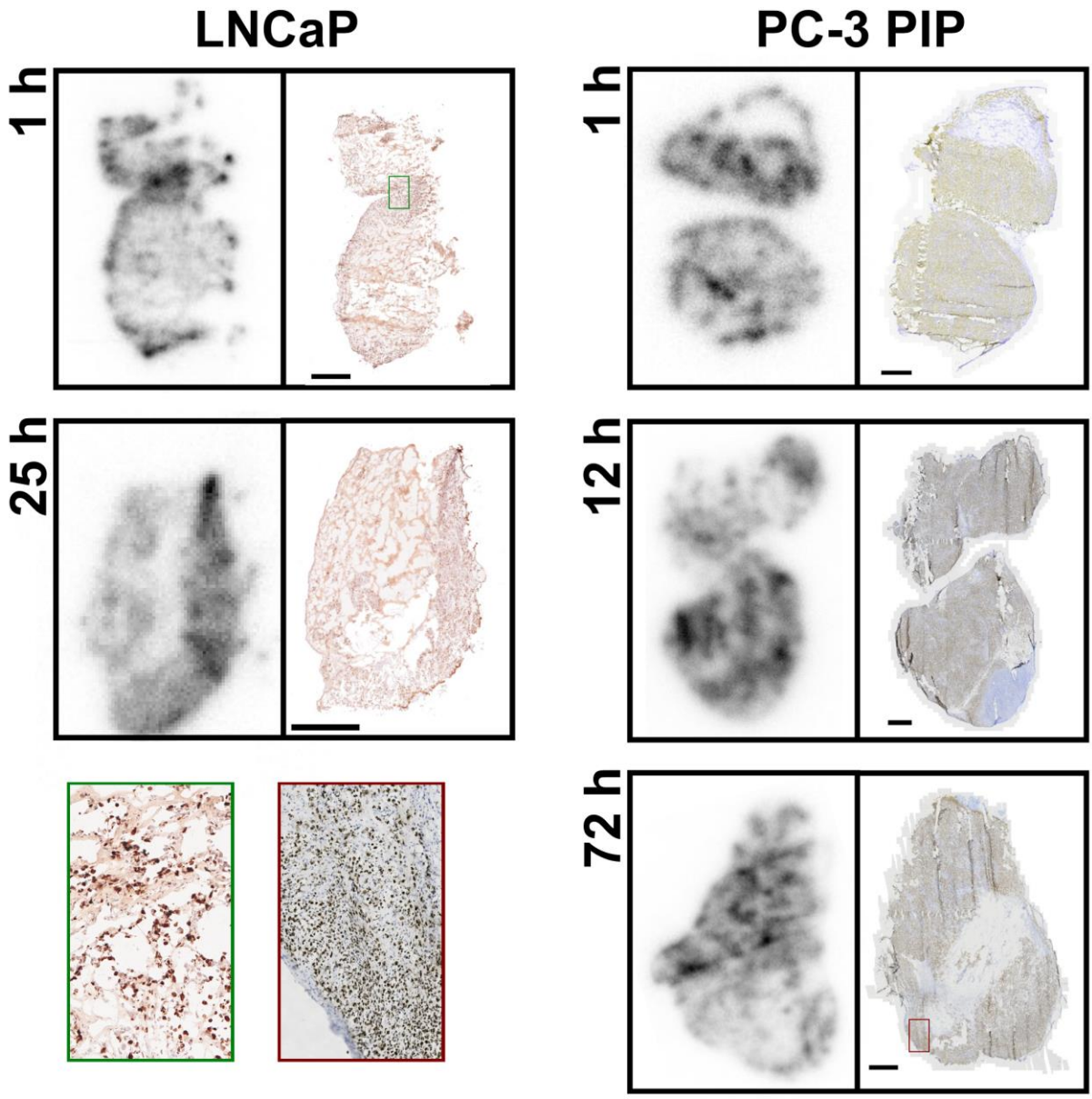


**FIGURE 2. Autoradiography and Ki67**

Autoradiography of [$^{177}$Lu]Lu-PSMA-617 uptake (left), and IHC of the proliferative marker Ki67 in an adjacent section (right). Note 1 h p.i. with a magnified high uptake, high Ki67, area marked in green, and 72 h p.i. with a magnified low uptake, high Ki67, area marked in red. All autoradiography images are individually scaled from zero (white) to max uptake (black) in that image. Black horizontal lines represent 1 mm.

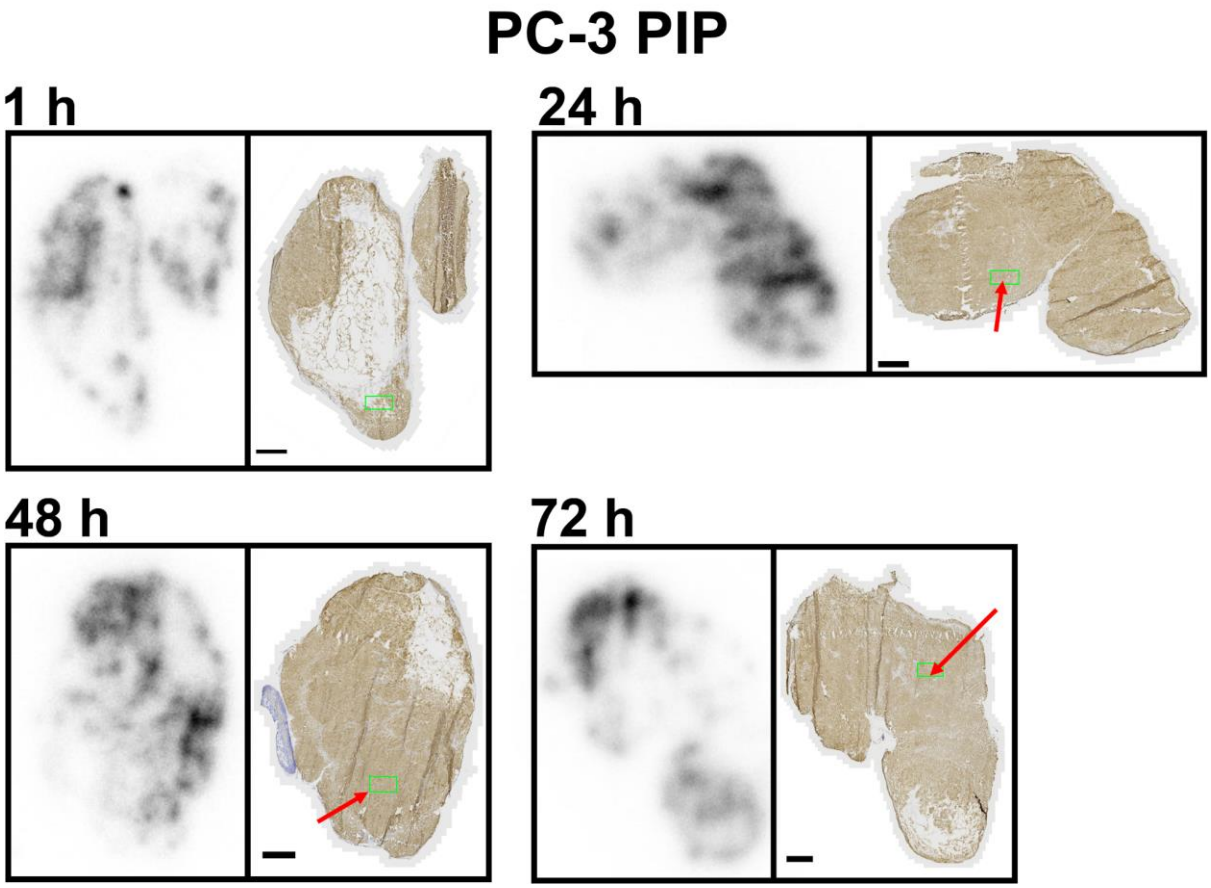


**FIGURE 3. Autoradiography and PSMA**

Autoradiography of [$^{177}$Lu]Lu-PSMA-617 uptake (left), and IHC of the target antigen PSMA in an adjacent section (right), in PC-3 PIP xenografts. Red arrows indicate areas of PSMA expression but low [$^{177}$Lu]Lu-PSMA-617 uptake. Green regions have PSMA staining quantified in Supplementary materials. All autoradiography images are individually scaled from zero (white) to max uptake (black). Black horizontal lines represent 1 mm.

# LNCaP

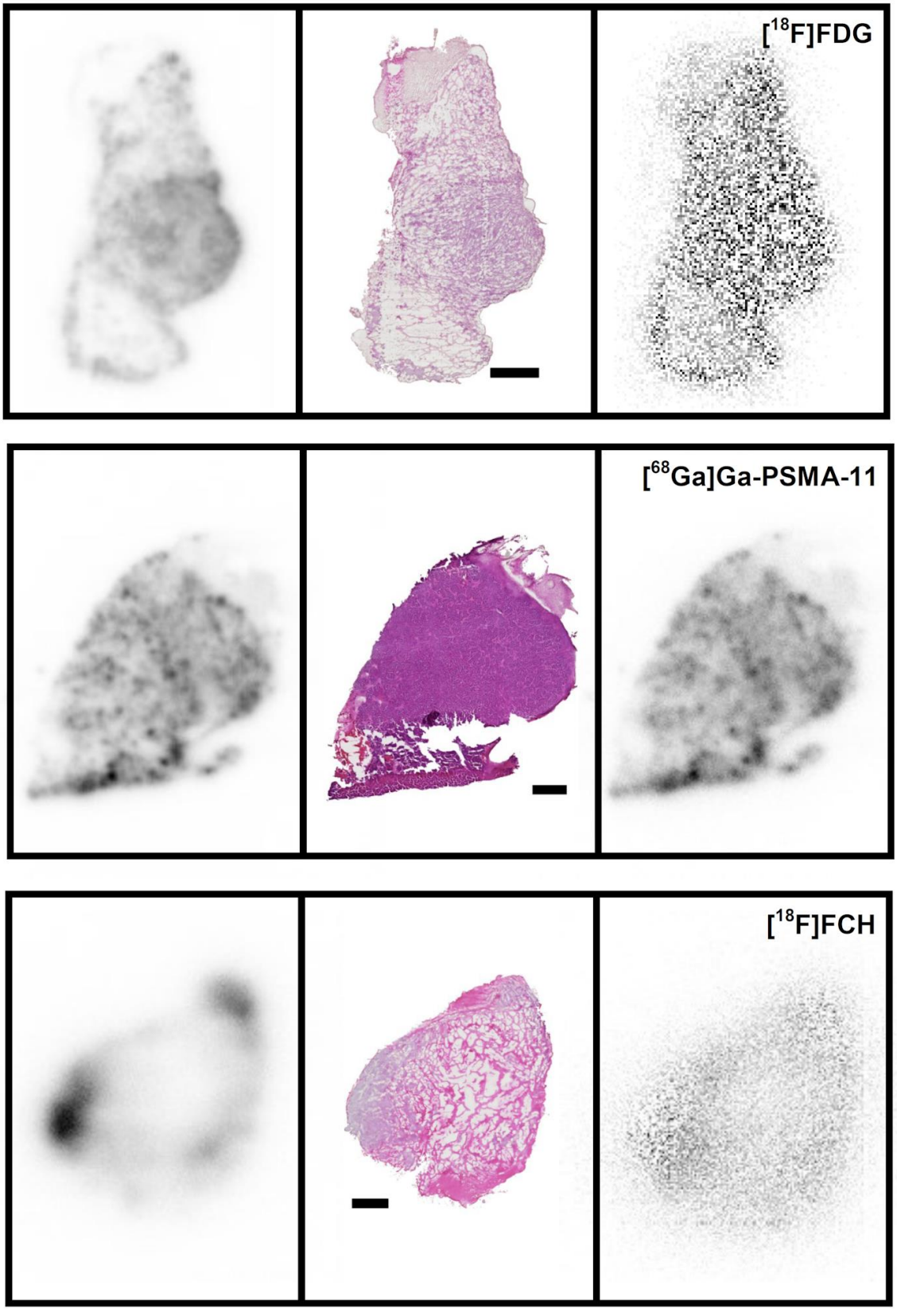

**FIGURE 4. Autoradiography, histology, and diagnostic tracers**

Autoradiography of [$^{177}$Lu]Lu-PSMA-617 uptake (left), H&E staining of histology (middle), and autoradiography of a diagnostic tracer (right), all three images per row are of the same section. LNCaP xenografts 1 h p.i. All autoradiography images are individually scaled from zero (white) to max uptake (black) in that image. Black horizontal lines represent 1 mm.

# Electronic Supplementary Material

## Tumor size measurements

For some animals with PC-3 PIP xenografts injected with 12-22 MBq [$^{177}$Lu]Lu-PSMA-617, tumor sizes were measured with calipers at injection and sacrifice at 1 day p.i. (n=2), 2 day p.i. (n=3), and 3 day p.i. (n=3). Results (Figure Supplementary 6) show that even though we see an immediate reduction in size at 1 day p.i. on 2 and 3 day p.i. several measurements are close to the size on injection day which could be interpreted as a simultaneous process of reduction through therapeutic effect and growth of new areas, consistent with our other results.

Also consistent with our results are the tumor sizes measured in our published study (Kristiansson et al. 2021) where similar animals as in this study, with LNCaP xenografts from the same original cell line and inoculated in the same manner, received 100 MBq of [$^{177}$Lu]Lu-PSMA-617 labelled in the same manner[46]. In that study we saw a reduction in average tumor size for approximately the first three weeks p.i. followed by regrowth, which would match our results showing small new grown areas without activity uptake in LNCaP tumors at 2 and 3 weeks p.i.

## Additional correlation analysis

The correlation between the level of relative uptake/activity (counts in each pixel as fraction of the maximum counts found in a pixel in each section) and cell proliferation (Ki67 staining) was evaluated in some LNCaP tumors. This was done by comparing the mean uptake in regions-of-interest (ROIs). ROIs between 0.09 and 1.66 mm$^2$ in size was drawn on areas of different uptake using ImageJ with identical ROIs in the adjacent Ki-67 stained slide drawn

using ZEN 3.5 blue edition software (Carl Zeiss AG,). The Ki67 ROIs were exported and opened in ImageJ.

These sections had some issues with low intensity hematoxylin staining and non-specific DAB color in the background so before analysis the method was calibrated against a sample. To achieve correct quantification the blue channel was amplified, and contrast raised in the same amount for all images before analysis.

Intensity of staining per nuclear area was determined using the Immunoratio plugin for ImageJ with default settings apart from -50 brown threshold and -10 blue threshold. Statistical analysis was performed separately for the 1 hour time post injection timepoint and a bundled timepoint for 2-3 weeks post injection using IBM SPSS Statistics version 27 (IBM, Armonk, NY, USA). Both the parametric Pearson correlation and the non-parametric Spearman's correlation were calculated. Results below.

**Correlation between relative [$^{177}$Lu]Lu-PSMA-617 uptake and fraction of cells with Ki67 staining in LNCaP tumor sections**

| Time post injection | 1 h | 2-3 weeks |
|---|---|---|
| Number of ROIs analyzed | 17 | 10 |
| Pearson Correlation | 0.675* | -0.438 |
| Spearman's Correlation | 0.664* | -0.515 |

* Correlation is significant at the 0.01 level (2-tailed).

**Analysis of PSMA IHC staining**

To illustrate the development of higher PSMA positive IHC staining in areas of low relative [$^{177}$Lu]Lu-PSMA-617 uptake in PC-3 PIP tumors over time, regions of the PSMA IHC images in Figure 3 were quantified in the same manner as for Ki67. This was gain done using the Immunoratio plugin for ImageJ with default settings apart from -25 brown threshold and +15 blue threshold. Results below.

**Measurement of the fraction of cells with PSMA staining in low-relative uptake regions marked in green in PC-3 PIP tumor sections displayed in Figure 3.**

| Time post injection | 1 h | 24 h | 48 h | 72 h |
|---|---|---|---|---|
| Fraction of cells with PSMA staining | 76.0% | 85.1% | 86.1% | 90.9% |

**Supplementary figures**

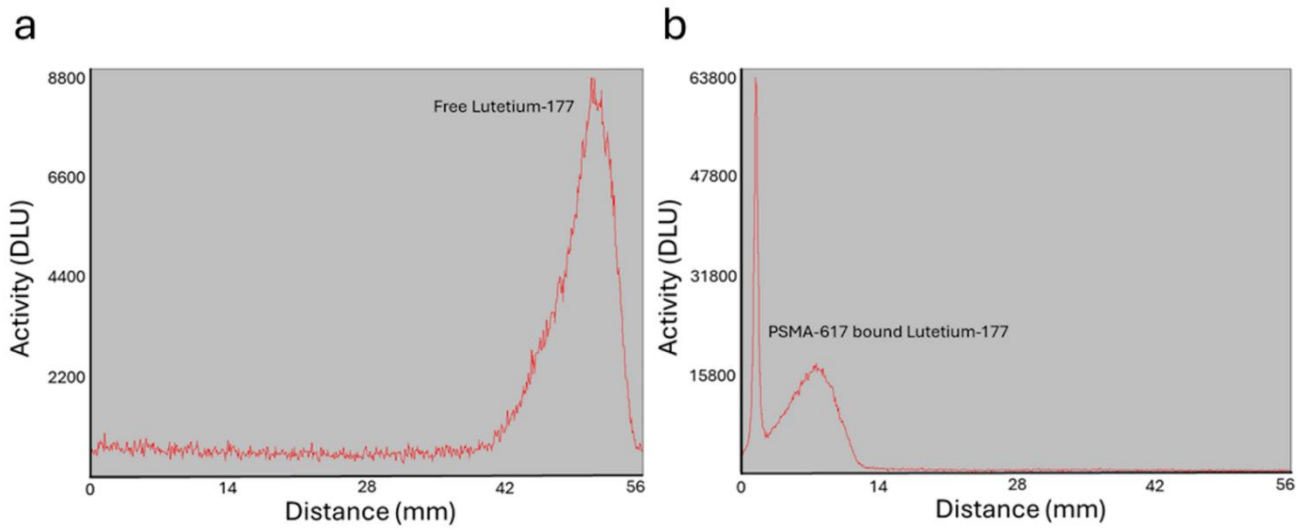


**Figure Supplementary 1. Instant Thin Layer Chromatography (iTLC) trace acquired with a Cyclone Plus Phosphor Imager for free Lutetium-177 and PSMA-617 complexed Lutetium-177.**

In saline solution, free Lutetium-177 (**a**) migrate with the solvent up the iTLC strip whereas Lutetium-177 labeled PSMA-617 (**b**) stay at the bottom of the iTLC strip. Activity measured as digital light units (DLU)

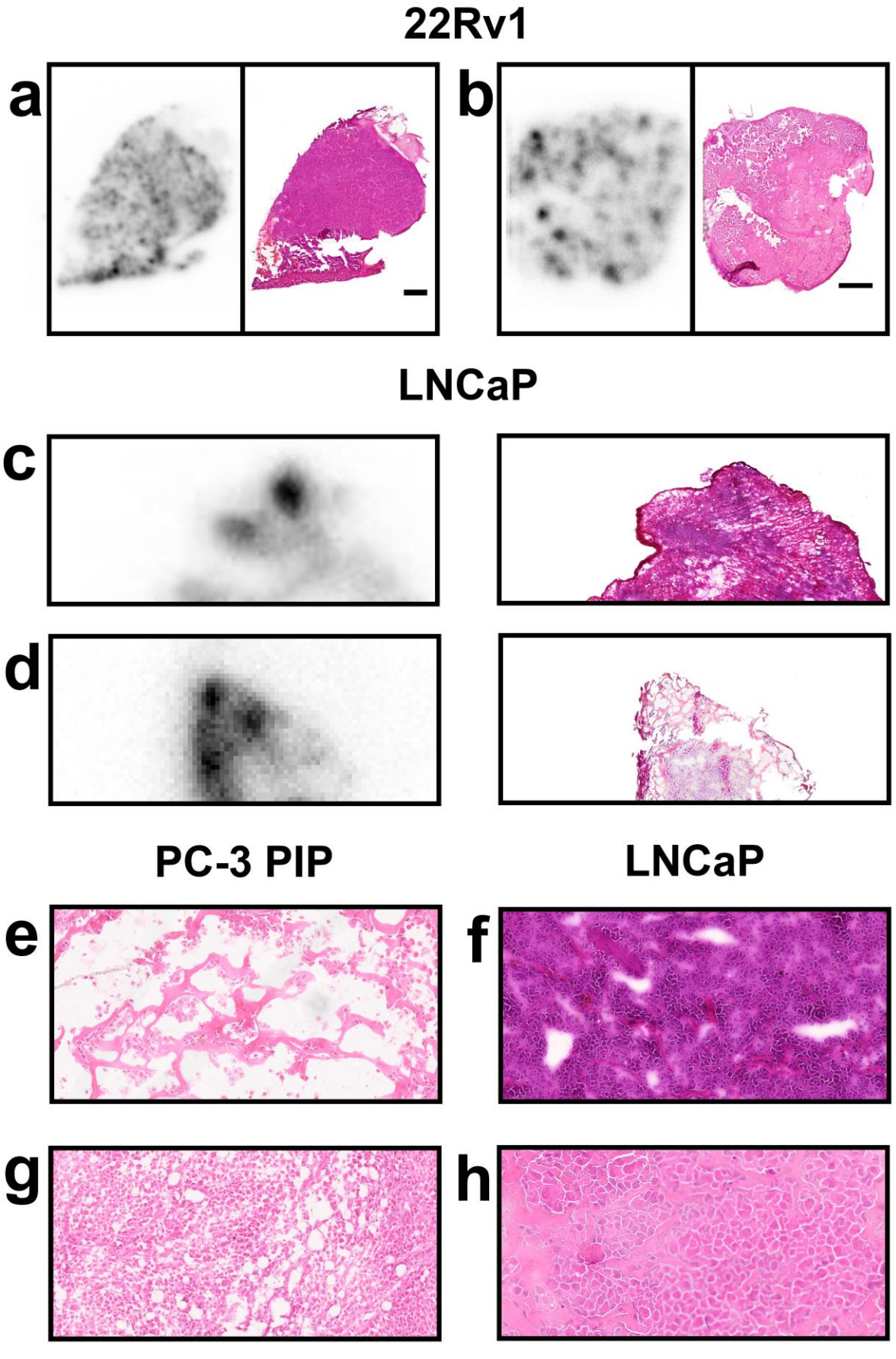
22Rv1
a
b
LNCaP
c
d
PC-3 PIP
LNCaP
e
f
g
h

**Figure Supplementary 2. Autoradiography and histology**

Autoradiography of [$^{177}$Lu]Lu-PSMA-617 uptake (left), and H&E staining of histology in the same section (right). 22Rv1 xenografts 1 h p.i. (**a**) and 2 h p.i. (**b**). Magnified images of sections from LNCaP xenografts also shown in Figure 1. 90 min p.i. (**c**) and 3 weeks p.i. (**d**). Magnified H&E images from Figure 1. Area A, necrotic tissue in PC-3 PIP at 12 h p.i. (**e**), area B, viable cells in LNCaP at 90 min p.i. (**f**), area C, binding tissue in PC-3 PIP at 24 h p. I (**g**), area D, viable cells in LNCaP at 2 weeks p.i. (**h**).

All autoradiography images are individually scaled from zero (white) to max uptake (black) in that image. Black lines represent 1 mm.

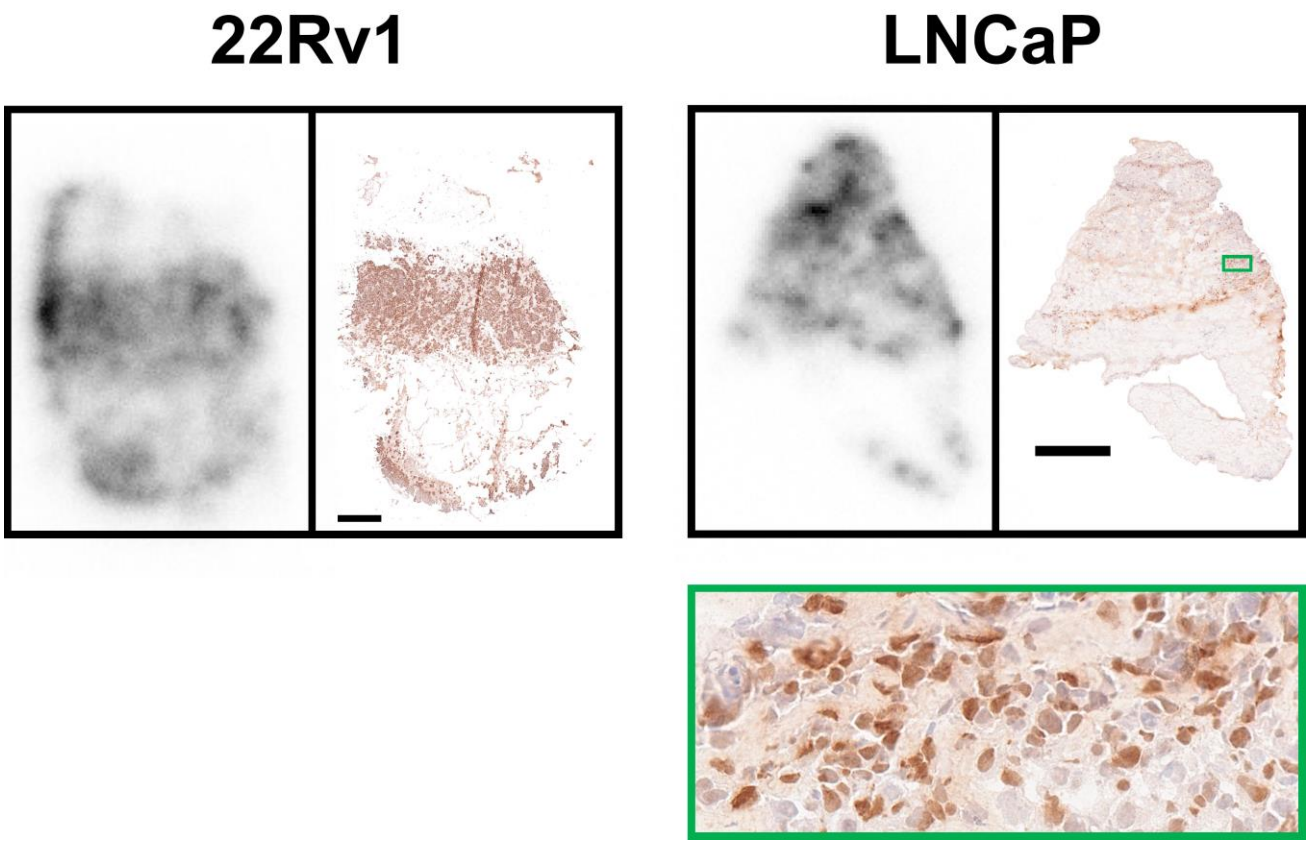


**Figure Supplementary 3 . Autoradiography and Ki67**

Autoradiography of [$^{177}$Lu]Lu-PSMA-617 uptake (left), and IHC of the proliferative marker Ki67 in an adjacent section (right). 22Rv1 xenograft 1 h p.i., LNCaP xenograft 2 weeks p.i. with a magnified area of low uptake, high Ki67 expression. Autoradiography images are individually scaled from zero (white) to max uptake (black). Black horizontal line represent 1 mm.

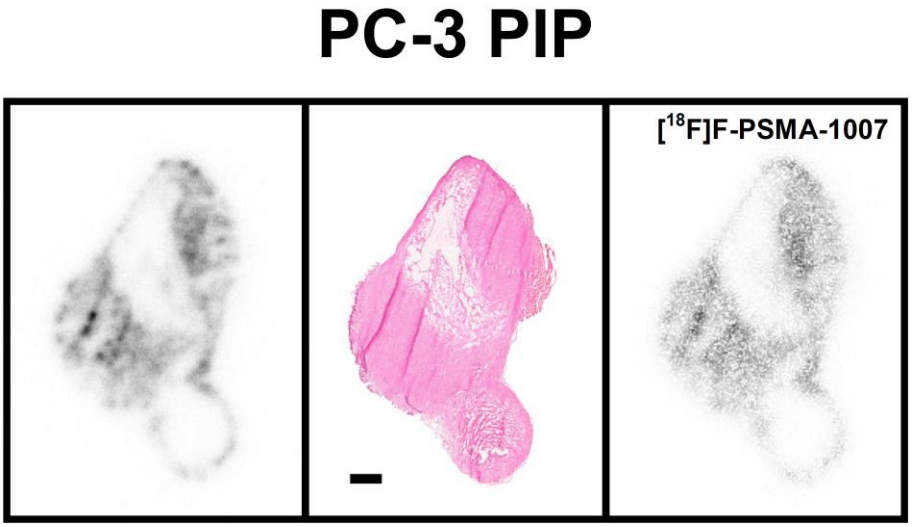


**Figure Supplementary 4. Autoradiography, histology, and diagnostic tracers**

Autoradiography of [$^{177}$Lu]Lu-PSMA-617 uptake (left), H&E staining of histology (middle), and autoradiography of a diagnostic tracer (right), all three images are of the same section. PC-3 PIP xenograft 1 h p.i. All autoradiography images are individually scaled from zero (white) to max uptake (black) in that image. Black horizontal line represents 1 mm.

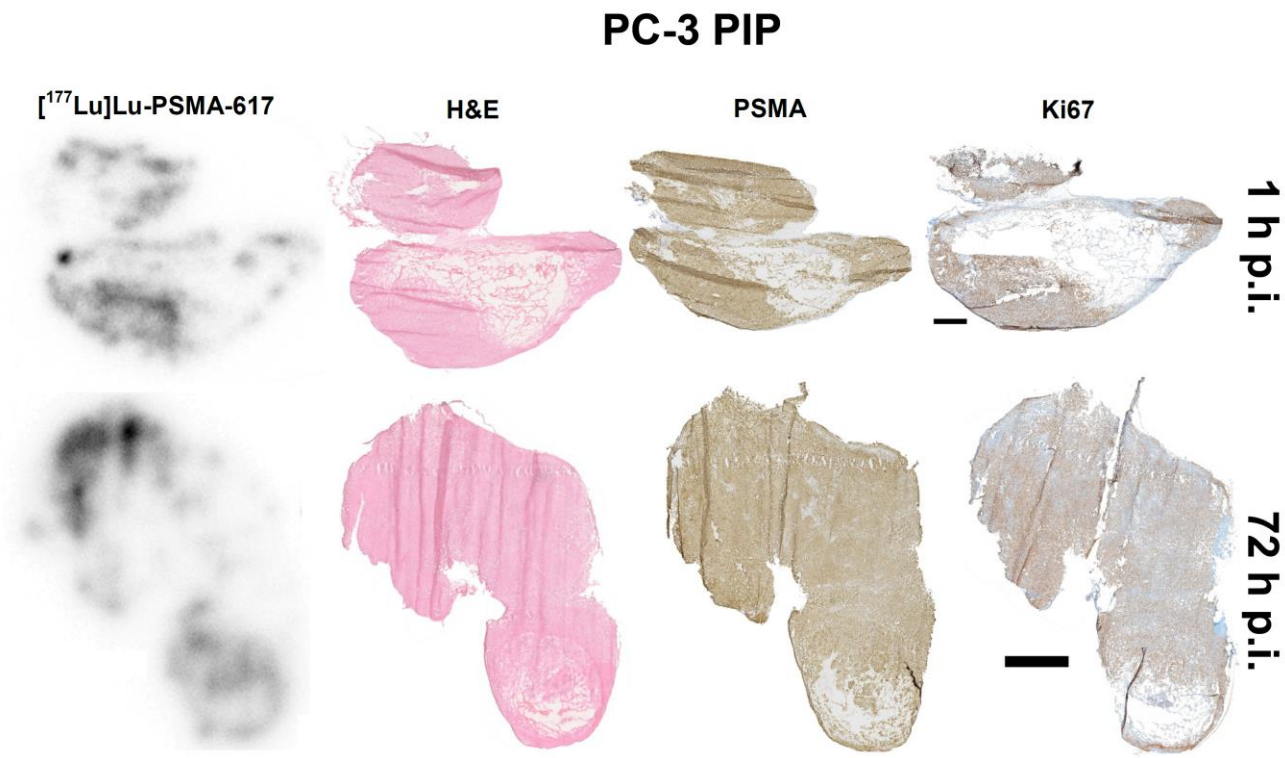


**Figure Supplementary 5. Combined illustration of connection between uptake, histology and expression of PSMA and Ki67.**

Autoradiography of [$^{177}$Lu]Lu-PSMA-617 uptake, H&E staining of histology (in the same section) and IHC of PSMA and Ki67 (in adjacent sections) in sections of PC-3 PIP xenografts at two timepoints. All autoradiography images are individually scaled from zero (white) to max uptake (black) in that image. Black horizontal lines represents 1 mm.

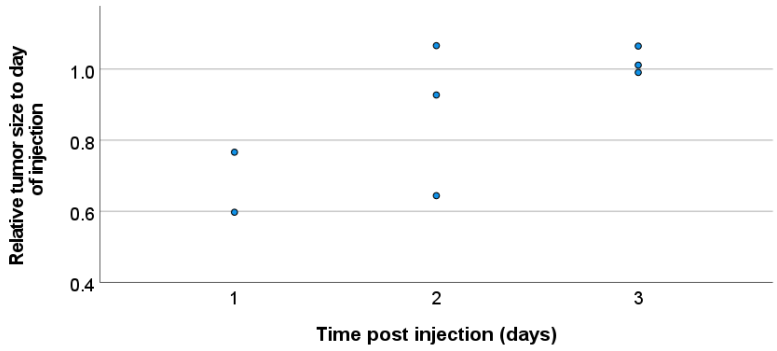


**Figure Supplementary 6. Relative tumor size to day of injection for PC-3 PIP tumors.**

Tumor sizes were measured at injection and sacrifice for some animals with PC-3 PIP xenografts injected with 12-22 MBq [$^{177}$Lu]Lu-PSMA-617 and relative tumor size calculated.

## References

46. Kristiansson A, Örbom A, Ahlstedt J, et al. 177Lu-PSMA-617 therapy in mice, with or without the antioxidant α1-microglobulin (A1M), including kidney damage assessment using 99mTc-MAG3 imaging. *Biomolecules.* 2021;11(2):263; doi: 10.3390/biom11020263